Dynamics of femtosecond-laser-induced lateral motion of an adsorbate: O on vicinal Pt(111)

2006 J. Phys.: Condens. Matter 18 S1409

(http://iopscience.iop.org/0953-8984/18/30/S04)

INSTITUTE OF PHYSICS PUBLISHING JOURNAL OF PHYSICS: CONDENSED MATTER

J. Phys.: Condens. Matter **18** (2006) S1409–S1424 doi:10.1088/0953-8984/18/30/S04

Dynamics of femtosecond-laser-induced lateral motion of an adsorbate: O on vicinal Pt(111)

J Güdde and U Höfer

Fachbereich Physik und Zentrum für Materialwissenschaften, Philipps-Universität, D-35032 Marburg, Germany

E-mail: Jens.Guedde@physik.uni-marburg.de

Received 31 December 2005
Published 14 July 2006
Online at stacks.iop.org/JPhysCM/18/S1409

Abstract

For the system of oxygen adsorbed at the step sites of a vicinal Pt(111) surface it has been demonstrated that diffusion of strongly bound atomic adsorbates can be induced electronically with femtosecond laser pulses (Stépán *et al* 2005 *Phys. Rev. Lett.* **94** 236103). The dynamics of energy transfer between the initial electronic excitation of the metallic substrate and the adsorbate motion is examined by comparing experimental hopping rates with those obtained from different model calculations. For this purpose the adsorbate–substrate coupling is approximated by an electronic friction. The experiment shows a strong nonlinear dependence of the hopping rate on laser fluence (F^{15}) and a coupling time of 1.5 ps between electronic excitation and diffusive motion as deduced by two-pulse correlation measurements. The consistent modelling of these findings requires the introduction of a friction coefficient that strongly depends on electron temperature. This result is interpreted in terms of an indirect excitation mechanism. It is proposed that anharmonic coupling between primarily excited perpendicular O–Pt vibrations and frustrated translations results in an effective coupling strength that increases with increasing electron temperature.

(Some figures in this article are in colour only in the electronic version)

1. Introduction

The key for a microscopic understanding of electronically induced surface reactions is knowledge about the pathways and the dynamics of energy transfer from the initial electronic excitation to the nuclear motion of the adsorbate. In contrast to photochemical reactions in the gas phase, the coupling of an adsorbate to the substrate introduces additional channels for this energy transfer. On the one hand, this generally leads to delocalization and enhanced dissipation of the excitation energy and thus to drastically reduced reaction efficiencies as recognized very early by Menzel, Gomer and Redhead [1, 2]. On the other hand, the strong

coupling extends the possibilities to initiate surface reactions because the creation of hot electrons or holes in the substrate is in turn able to cause adsorbate motion [3–5]. Ultra-short laser pulses offer unique capabilities, both for initiating and analysing such types of surface reactions. Femtosecond lasers not only allow us to study the energy transfer dynamics on the timescale of nuclear motion directly in the time domain, but they also hold promise for a certain amount of control of adsorbate motion before the excitation energy is thermalized within the whole adsorbate–substrate system.

In the past, experiments that exploited these opportunities of femtochemistry at surfaces have mainly concentrated on desorption phenomena of small molecular adsorbates from metal surfaces [6–24]. Typically, these experiments showed reaction yields that were many orders of magnitude higher than those of conventional photochemical reactions at metal surfaces [3, 25, 26] as well as a nonlinear dependence of the yield on laser fluence. In contrast to the usual process of desorption induced by electronic transitions (DIET) where the reaction is initiated by single Franck–Condon transitions [1, 2], the high density of electron–hole pairs created in the metal by intense femtosecond pulses typically causes repetitive electronic transitions between the ground and excited states of the adsorbate–metal system on the timescale of nuclear motion. Consequently, this new regime of desorption induced by multiple electronic transitions has been named DIMET [27]. In many cases, a basic understanding of the electronic excitation of adsorbate motion can be achieved by models that do not consider the multitude of individual transitions but describe the non-adiabatic coupling between the electronic system of the metal substrate and the adsorbate degrees of freedom by electronic friction [28–34]. Time-resolved studies have taken advantage of the nonlinear fluence dependence by applying a two-pulse correlation scheme [7] for the determination of the energy transfer time from the electronic excitation to the adsorbate degrees of freedom. They allow us to make a clear distinction between electronic and phononic energy transfer [11, 18].

In this paper we will report on an extension of these DIMET studies to diffusion processes of adsorbates. Diffusion is an important elementary step of many surface processes such as epitaxial growth or catalytic reactions. Usually, surface diffusion is a thermally activated process that is initiated by heating the substrate. At sufficiently high temperature the thermal population of frustrated translations or rotations enables a small fraction of the adsorbates to overcome the barrier E_{diff} for lateral motion and to hop to the next adsorption site. This process requires a minimum temperature of the order of $kT \approx E_{\mathrm{diff}}/20$, and it generally strongly favours the diffusion pathway with the lowest barrier height over any other one. In some cases it would be desirable to have more control over migration pathways or to enable diffusion of a particular species at a lower temperature where competing surfaces reaction have not yet set in. For these and other purposes one would like to induce diffusion by electronic instead of thermal excitation of the adsorbate–substrate. From an energetic point of view, lateral motion is easier to excite than desorption since diffusion barriers are generally much lower than chemisorption energies. Similarly, one can expect that the amount of electronic excitation required to initiate diffusion should be less than the amount required for desorption. In fact, the concept of electronic friction to describe the electronic coupling of an adsorbate with a metal surface was first discussed in the context of diffusion [35, 36].

Experimentally, however, the observation of lateral motion following electronic excitation is more difficult to detect than desorbing atoms or molecules in the gas phase. Bartels and co-workers used scanning tunnelling microscopy (STM) for this purpose [37]. In case of CO/Cu(110), they were able to show that electronic excitation of the substrate induced by absorption of short laser pulses gives rise to diffusion of CO parallel and perpendicular to the close-packed rows, while thermal excitation leads to diffusion only along the rows [37]. In our study we employed the sensitivity of second-harmonic generation (SHG) on surface symmetry

to monitor fs-laser-induced diffusion of atomic oxygen from step sites onto the terraces of a vicinal Pt(111) surface *in situ* and in real time [38]. While this technique cannot detect individual hopping events, it has advantages in terms of extracting time-domain information, which usually requires averaging over individual events [39]. Systematic studies of the hopping rate for step-terrace diffusion as a function of fluence and delay time of two pump laser pulses by Stépán *et al* [38] clearly showed that the diffusion process is driven by the laser-excited electrons and not meditated by substrate phonons. The idea of employing a vicinal Pt surface to distinguish between different adsorption sites was also used by Backus *et al* [40]. In their time-resolved sum-frequency generation experiment it is the different stretch frequency of CO adsorbed at step and terrace sites that allowed them to monitor lateral motion.

In the following we will first review our recent experimental results for laser-induced diffusion of oxygen on vicinal Pt(111). They show the same characteristics as found in laser-induced desorption experiments for systems which are dominated by electronic coupling: a strong nonlinear dependence of the hopping rate on laser fluence and a narrow two-pulse correlation. In section 3 we then discuss the electronic excitation mechanism of adsorbate diffusion induced by fs-laser excitation. We will compare model calculations performed with different variants of electronic friction models for an approximate description of the coupling between adsorbate and substrate degrees of freedom. Our results show that, in contrast to laser-induced desorption experiments, the consistent modelling of our experimental results requires the introduction of an electronic friction coefficient that increases with the electron temperature of the substrate. This result is not expected from the electronic structure of O/Pt. It suggests that the dependence of the electronic friction on electron temperature is only an effective one and is in fact connected to a more complicated energy transfer mechanism between electronic excitation and nuclear motion. We propose that the frustrated translation of the adsorbate is excited predominantly by indirect anharmonic coupling to the perpendicular O/Pt vibration.

2. Experimental results

Our choice of atomic oxygen on a vicinal Pt(111) surface for the study of laser-induced diffusion is motivated by its model character for diffusion of a strongly chemisorbed atomic adsorbate and for experimental reasons. Due to the importance of Pt as a catalyst in oxidation reactions the dissociative adsorption of O_2 on Pt has been well characterized by a variety of methods (see for example [41, 42] and references therein). Steps increase the reactivity of the substrate dramatically [42–44] and STM investigations at temperatures lower than 160 K, where atomic oxygen is immobile, have shown that the dissociative adsorption takes place directly at the step edges [45]. This makes it possible to easily generate a well defined initial distribution of oxygen atoms which occupy all available step sites. Hopping from step sites onto the initially empty terraces was induced by absorption of femtosecond laser pulses as sketched in the inset of figure 1. The relatively large diffusion barrier ensured that diffusion was only induced by the laser pulses and not initiated by thermal activation at a temperature of 80 K. The depopulation of the step sites was monitored by optical second-harmonic generation (SHG) that owes part of its sensitivity to the occurrence of a symmetry break at surfaces [46, 47]. Since the presence of regular steps on a vicinal surface breaks the symmetry parallel to the surface, step sites can be a very efficient source of SHG [48–50]. The capability of SHG to monitor step coverage *in situ* and in real time allowed for the determination of diffusion rates as a function of laser fluence and delay between two pump pulses.

The experiments were performed in ultra-high vacuum at a base pressure of $<1 \times 10^{-10}$ mbar with a Pt crystal miscut by 4° from the (111) plane in the $[1\bar{1}0]$ direction. The resulting (10, 12, 11) surface consisted of 12 unit cell wide terraces and step edges along the $[11\bar{2}]$

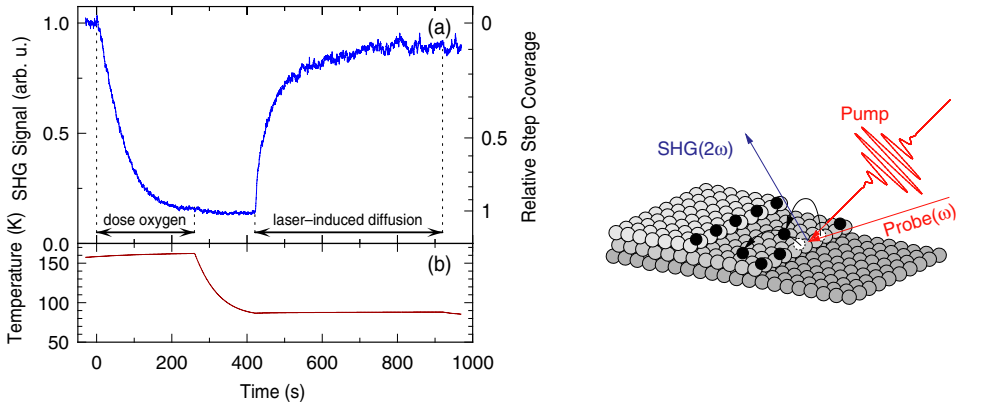

Figure 1. Second-harmonic signal (a) and temperature (b) as a function of time. First, oxygen is dosed at a temperature of 160 K. After cooling to 80 K, diffusion is induced by applying the pump laser with an absorbed fluence of 5.6 mJ cm^{-2} at a repetition rate of 1 kHz, leading to a recovery of the SH signal due to the depopulation of the step edges. Reproduced from [39]. Copyright 2005, Elsevier B.V. The scheme on the right sketches the optical excitation by an intense femtosecond pump pulse and the monitoring of the step coverage by SHG.

direction (compare reference [51]). The sample was attached to a liquid-nitrogen cryostat at a base temperature of 80 K. It could be heated up to 1100 K by radiation and electron-beam heating. A gas-dosing system allowed for the exposure of controlled amounts of research grade oxygen through a micro-channel plate. Sample preparation has been done by standard sputter–anneal cycles and oxygen treatment at 720 K followed by flash desorption of the oxygen at 1100 K. Surface cleanness and order has been verified by LEED/Auger and temperature-programmed desorption (TPD) of oxygen. In particular, the reproducibility of the TPD spectra [39] for recombinatively desorbed oxygen is a very sensitive probe of surface cleanness since even small amounts of contamination strongly suppress dissociated adsorption. Diffusion was induced by 50 fs pulses from a kHz Ti:sapphire amplifier system operating at 800 nm. The output was split into two orthogonally polarized beams, combined collinearly with variable time delay, incident on the sample at 40° from the surface normal and slightly focused to a spot of 1 mm in diameter. Femtosecond laser pulses at 800 nm were also used as the fundamental radiation for SHG. The SHG probe beam was p polarized and incident at 45° in a plane parallel to the step edges. The spot size was 10 times smaller than that of the pump beam, and the absorbed fluence of the probe pulses was kept below 0.5 mJ cm^{-2} in order to exclude any influence on the diffusion process. Detection of the p-polarized component of the second-harmonic radiation results in an SHG signal that originates predominantly from the steps. Further details of the experimental set-up are described in [39].

Figure 1(a) shows typical raw SHG data as a function of time during dosage and induced diffusion of oxygen. First, the sample was kept at 160 K and exposed to constant flux of molecular oxygen. At this temperature, chemisorbed O_2 is not stable on the terraces. It desorbs or it diffuses to the step edges, where it preferentially dissociates and forms strongly bound atomic oxygen on top of the step edges [45]. Filling of the step sites with atomic oxygen leads to a strong reduction of the SHG signal until the steps are saturated ('dosing' regime in figure 1). This strong reduction with oxygen coverage demonstrates the high sensitivity of the SHG detection, even for a low step density of $1/12$. The monotonic decrease of the SHG signal makes it possible to relate the SHG signal to the relative coverage of the step sites θ_s (right scale in figure 1) using a simple model for the coverage dependence of the nonlinear

susceptibility [39]. Following step decoration of the sample with atomic oxygen, the sample was cooled down to 80 K, where oxygen is immobile even on the terraces. Partial depletion of the steps by thermal diffusion has been observed for sample temperatures exceeding 260 K. After reaching 80 K the sample was irradiated with femtosecond laser pulses at a repetition rate of 1 kHz ('laser-induced diffusion' regime in figure 1). We have observed a continuous recovery of the SHG signal for pulses that exceed an absorbed fluence of 3.5 mJ cm^{-2}. The recovery of the SHG signal is due to the depletion of the step sites by oxygen diffusion onto the terraces and not due to desorption. When we scan the spot of the pump beam with a fluence of 6 mJ cm^{-2} slowly over the whole sample surface, subsequently recorded temperature-programmed-desorption (TPD) spectra show no indication of a laser-induced decrease of the total oxygen coverage. Since thermal desorption of atomic oxygen takes place recombinatively around 800 K, i.e. at a much higher temperature than diffusion, we expect that laser pulses exceeding the damage threshold of the sample would be required to induce desorption with our experimental set-up. The fact that we observe almost complete step depletion at higher laser fluences indicates that the laser-induced diffusion process is not defect mediated but affects all step sites.

The saturation of the SH signal for large times below the initial value reflects the equilibrium distribution of oxygen at steps and on terraces under conditions of intense laser excitation. In thermal equilibrium, the ratio between step- and terrace-bound O atoms depends on the temperature and on the difference between the binding energy for step and terrace sites. At first glance one would expect a rather large energy difference, since oxygen binds preferentially at the step edges even at room temperature [45, 52]. However, the decoration of the step edges is primarily due to the enhanced reactivity for dissociative adsorption at the step edges and does not require any difference in the binding energies as long as the establishment of a thermal equilibrium distribution is hindered by a large enough diffusion barrier. First-principles calculations [52] for 2×1 superlattices of O on Pt(211) and Pt(322) yielded a binding energy difference of 0.4–0.6 eV between step- and terrace-bound O depending on step type. This difference is expected to be considerably lower when isolated O atoms on the terraces are considered. At saturation coverage the repulsive interaction between O atoms leads to a reduction of the adsorption energy by about 20% [43, 53]. The presence of a relatively small binding energy difference between step and terrace adsorption under our experimental conditions is supported by the fact that we can populate the terraces by thermal induced diffusion for temperatures around 300 K.

The step-selective detection of the SHG signal makes it possible to extract diffusion rates on an atomic scale, even though this optical technique averages over a large surface area. The quantity discussed in the following is the hopping probability p_{dif} per laser shot for migration from the step sites onto the terraces. In principle, this quantity can be determined directly from the initial slope $\mathrm{d}\theta_{\mathrm{s}}/\mathrm{d}t$ of the SHG data recorded after switching on the pump pulses. The data shown in figure 1 have roughly an initial slope of $\mathrm{d}\theta_{\mathrm{s}}/\mathrm{d}t \approx -0.5/10$ s, which gives $p_{\mathrm{dif}} \approx 5 \times 10^{-5}$ for a repetition rate of 1 kHz. In order to exploit the excellent statistics of the whole data sets we have determined p_{dif} by describing the diffusion kinetics using a simple one-dimensional rate equation model [39]. We note that with our method of continuously monitoring the step coverage with SHG we achieve an accuracy for the determination of laser-induced diffusion rates that is comparable with or even higher than the best measurements of desorption rates using QMS detection [12, 15, 18].

One characteristic feature of experiments in the DIMET-regime is a nonlinear dependence of the yield on laser fluence, which has been attributed to the repetitive electronic excitation [27]. In contrast, a single nonthermal excitation process is characterized by a linear fluence dependence [14]. Figure 2(a) displays several sets of raw SHG data during

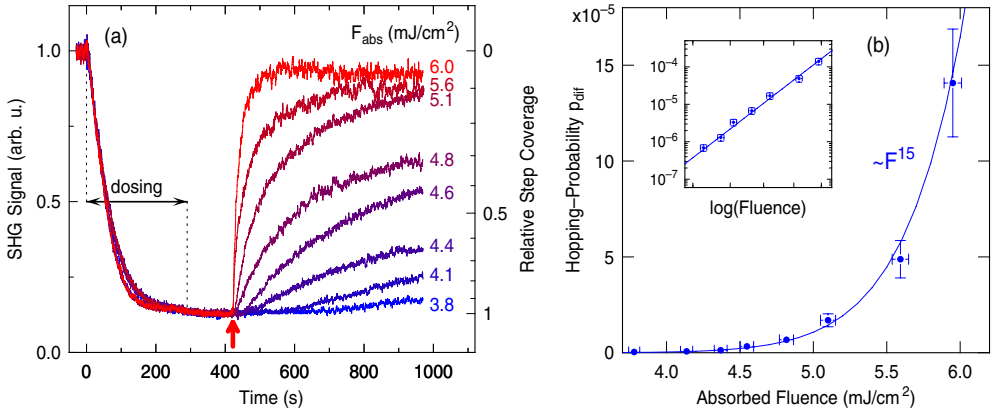

Figure 2. (a) Second-harmonic response of the Pt sample during dissociative adsorption of O_2 at the steps (dosing) and diffusion of atomic oxygen induced by femtosecond laser pulses of various absorbed fluences F_{abs}. The pump pulses had a repetition rate of 1 kHz and were switched on at the time marked by the vertical arrow. The right y-scale gives the conversion of the SHG signal into the relative step coverage [39]. Reproduced from [38]. Copyright 2005, The American Physical Society. (b) Hopping probability per laser shot p_{dif} for the diffusion of oxygen from the filled step sites onto the empty terraces as a function of absorbed laser fluence F. The inset shows the data in a logarithmic scale. The solid line shows a power law $\propto F^{15}$.

oxygen dosage and induced diffusion for various absorbed fluences. It demonstrates the high reproducibility of the experiment and the strong dependence of the diffusion rate on laser fluence. Variation of the laser fluence by only 50% covers the whole accessible dynamic range of the diffusion rate. Plotting the initial hopping probability per laser shot p_{dif} as a function of absorbed fluence reveals an extremely strong nonlinear fluence dependence (figure 2(b)). In the investigated fluence range it can be described by a power law of the form $p_{dif} \propto F^x$, as is the case for the desorption probability in most of the femtosecond desorption experiments. However, the nonlinearity shown here with $x = 15$ is much stronger than in all laser-induced desorption experiments so far, where an exponent in the range of 3–8 has been typically observed [6, 10, 12, 15]. Even for such a strong nonlinearity, the factor-of-ten smaller spot size of the probe beam ensures that the yield is spatially uniform over the diameter of the probe beam within 10%. The nonlinear detection further narrows the effective probe diameter by a factor of $\sqrt{2}$, which finally reduces the non-uniformity to 5%. Thus, yield averaging of the laser fluence [15] is not necessary here.

The assignment of an electronically induced diffusion process requires knowledge about the pathway of the energy transfer from the optically excited electrons to the diffusive motion. This has been revealed by the application of a two-pulse correlation scheme which was first applied to laser-induced desorption by Budde *et al* [7]. For this purpose, the pump pulse is split into two pulses with a variable time delay. Only for delays in which the system retains memory of the first excitation can the second pulse generate an enhanced yield compared to independent excitations. As in nonlinear optics, this requires a nonlinear dependence of the reaction yield on the laser fluence. The width of such a two-pulse correlation provides information about the timescale of the energy transfer from the initial excitation of the electrons to the adsorbate motion and allows the distinction between an electron- and a phonon-mediated process. A transfer time of less than a few picoseconds indicates a direct energy flow from the excited electrons to the adsorbate degree of freedom, whereas a coupling via the phonon system is characterized by a transfer time that is one order of magnitude longer [18].

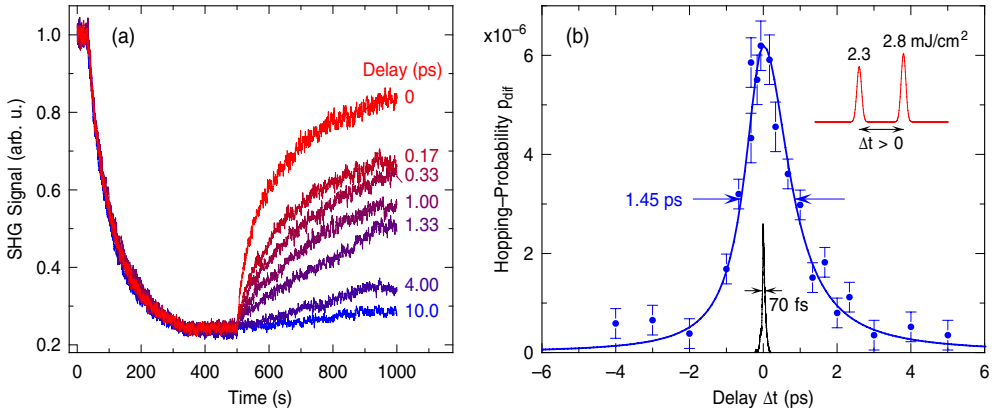

Figure 3. (a) Second-harmonic response during dosing and induced diffusion for different delays between two cross-polarized pump-laser pulses. (b) Hopping probability per laser shot p_{dif} as a function of delay between the p- and s-polarized pump beams with absorbed fluences of 2.3 and 2.8 mJ cm^{-2}, respectively (symbols). At positive delays, the weaker excitation precedes the stronger one (inset). The thick solid line is a guide to the eye. The thin line shows the SHG cross-correlation of the two pump pulses generated at the sample surface. Reproduced from [38]. Copyright 2005, The American Physical Society.

Figure 3 shows the two-pulse correlation (b) together with a set of raw SHG data (a) for various delays between the two pump pulses. p_{dif} shows a large contrast between small and large delays, which is related to the high nonlinearity of the fluence dependence. The width of 1.45 ps (FWHM) is much larger than the cross-correlation of the two laser pulses and has the value of a typical electron–phonon coupling time. This unambiguously shows that the diffusive motion is directly driven by the laser-excited electrons of the metallic substrate and not by the phonon bath. The two pump beams were cross-polarized in order to suppress a coherent interaction around zero delay. However, even small deviations of the polarization alignment result in an enhanced hopping rate if the pump pulses are overlapping in time. This can be seen for the zero-delay curve in figure 3(a) (not shown in (b)). This might point to a contribution of a direct excitation of the adsorbate, which would result in a very narrow two-pulse correlation due to the short lifetime of adsorbate resonances. Direct excitation has been observed in photochemistry of molecular adsorbates using UV light [54, 55]. Polarization-dependent experiments, or better two-photon photoemission, could unambiguously identify this mechanism [56–58]. Here, we will focus the discussion on the indirect excitation due to the laser-excited hot-electron distribution, which is responsible for the transfer time of about 1.5 ps.

3. Model calculations

The two-pulse correlation as well as the fluence dependence of the hopping probability show the typical characteristics of a process which is induced by multiple electronic transitions. Thus, we have modelled fs-laser-induced diffusion within the same formalisms as used for the description of desorption. Typically, an indirect hot-electron excitation process for fs-laser-excited surface reactions on metal surfaces is analysed in two steps. First, the dynamics of the laser-excited hot-electron distribution is described by applying the well known two-temperature model [59]. This model describes the energy flow between the electronic and phononic systems of the substrate by two coupled heat diffusion equations, which allows the assignment of time-

dependent electronic and ionic temperatures $T_e(t)$ and $T_i(t)$:

$$C_e \frac{\partial}{\partial t} T_e = \frac{\partial}{\partial z}\left(\kappa_e \frac{\partial}{\partial z} T_e\right) - g(T_e - T_i) + S(z,t) \tag{1}$$

$$C_i \frac{\partial}{\partial t} T_i = g(T_e - T_i). \tag{2}$$

Here, $C_e = \gamma T_e$ and C_i are the electron and ion heat capacities respectively. $\kappa_e = \kappa_0 T_e / T_i$ is the electronic thermal conductivity, and g is the electron–phonon coupling constant. Heat conduction by phonons can be neglected in metals in the temperature regime of interest. The term $S(z,t)$ describes the optical excitation of the electrons. Although it can take up to several hundred femtoseconds until the initial non-equilibrium energy distribution of the excited electrons transforms into a hot Fermi–Dirac distribution by electron–electron scattering [60–62], the assumption of an instantaneous thermalization is reasonable in most cases, since an indirect excitation of an adsorbate by hot electrons typically proceeds on the timescale of one picosecond, as indicated by the width of the corresponding two-pulse correlation.

Two principal models have been employed for the description of the second step, the energy transfer to the nuclear coordinates of the adsorbate. One is the DIMET model [27], which describes the excitation of the adsorbate by multiple electronic transitions between potential energy curves with high-lying adsorbate levels. It emphasizes the dynamics of the adsorbate on the excited potential energy surface (PES), from where it rapidly falls into the ground state due to the strong coupling to the surface. It is derived from the MGR model [1, 2] of the usual DIET Process, in which desorption occasionally occurs if a molecule remains sufficiently long on an antibonding PES. A description in the DIMET model is most advantageous if the adsorbate dynamics proceed most of the time on one of the PESs, and excitations are relatively rare. Despite the rapid progress in theory [63], however, most theoretical descriptions in the DIMET model have no predictive character due to the lack of parameter-free potential energy surfaces.

For an increasing number of excitation and de-excitation cycles by Franck–Condon transitions at a different distances from the surface, the electronic excitations lead to an effective vibrational heating in the ground state, which becomes more and more important for the desorption process. Within this limit, the DIMET model makes contact with the electronic friction model [28, 31–33], which treats the coupling between the adsorbate and the electrons via an effective electronic friction. It is based on the theory of vibrational damping of adsorbates by the creation of electron–hole pairs [64, 65], which is the inverse process of electronic excitation of adsorbate motion. It emphasizes the dynamics on the ground state PES perturbed by the excited electrons and is most suitable in the presence of low-lying excited states of the adsorbate–substrate system. However, both descriptions are closely related and describe the same physical processes from different points of view.

In the empirical friction model [29, 30], the adsorbate is treated as a harmonic oscillator which is coupled to the heat bath of the electrons via an electronic friction coefficient η_e. By applying a master equation formalism, a relation for the temporal evolution of the average vibrational energy of the form

$$\frac{\mathrm{d}}{\mathrm{d}t} U_a = \eta_e [U_e - U_a] \tag{3}$$

has been derived, where U_e and U_a are the energies of the oscillator in equilibrium with the electron temperature T_e and an adsorbate temperature T_a respectively

$$U_x = h\nu_a (\mathrm{e}^{h\nu_a / kT_x} - 1)^{-1}. \tag{4}$$

Here, ν_a is the frequency of the adsorbate vibration along the reaction coordinate. The friction coefficient η_e is normalized to the adsorbate mass M and can be regarded as the inverse of an electron–adsorbate energy transfer time $\tau_{ea} = 1/\eta_e$. It is related to the friction coefficient f of a classical velocity proportional friction force $F_e = -fv$ by $f = \eta_e M$ [28]. Coupling to the phononic system has been considered by adding a corresponding term to equation (3), which introduces an ion-adsorbate energy transfer time [15]. This term can describe contributions to the reaction dynamics which proceeds on a timescale of several picoseconds [11, 15], but can be neglected here due to the observation of a narrow two-pulse correlation. Solving equation (3) with the time-dependent electron temperature $T_e(t)$ derived from the two-temperature model gives, together with equation (4), the time-dependent adsorbate temperature $T_a(t)$ which describes the vibrational excitation of the adsorbate. For first-order kinetics, the reaction rate is then given by an Arrhenius-type expression as

$$R(t) = -\frac{d}{dt}\theta(t) = \theta(t)\nu_a e^{-E_a/kT_a(t)}, \tag{5}$$

where θ denotes the relative coverage of the available sites. Thus, the initial reaction probability for a single laser shot at small changes of the coverage ($\theta \approx 1$) is simply given by $p = \int \nu_a \exp(-E_a/kT_a(t))\,dt$.

Brandbyge *et al* have shown that both DIMET and friction regimes can be covered within a generalization of the electronic friction model [32]. They derived an analytic result for an spatially independent friction and a truncated harmonic oscillator potential of depth E_a for the description of the adsorbate–surface interaction in the electronic ground state. In this case, the adsorbate and electron temperatures are directly coupled by the electronic friction coefficient η_e

$$\frac{d}{dt}T_a(t) = \eta_e(t)[T_e(t) - T_a(t)]. \tag{6}$$

This relation can be formally derived from the high-temperature limit of equation (3) if $h\nu_a/kT_x \ll 1$ and therefore $U_x \approx kT_x$. In principle, η_e depends on time and space and has to be calculated by microscopic theories [31, 34, 66]. It has been shown that the friction coefficient has a weak dependence on temperature and therewith on time if the adsorbate resonance is broad and close to the Fermi level. This case corresponds to the theory of adsorbate vibrational damping. The DIMET limit of a high-lying and well defined affinity level, on the other hand, is characterized by a friction coefficient which is small at low temperatures and increases strongly if the electron temperature is large enough to populate significantly the adsorbate resonance [32]. For thermal energies kT_a which are small compared to E_a, the probability to overcome the barrier E_a is given in this formalism as the time integral over a rate

$$R(t) = \eta_e(t)\frac{E_a}{kT_a(t)}e^{-E_a/kT_a(t)}. \tag{7}$$

In our laser-induced diffusion experiment E_a corresponds to the diffusion barrier E_{dif} and $p_{dif} = \int R(t)\,dt$ gives the hopping probability per laser shot. It should be noted that, in contrast to the empirical friction model, η_e not only governs the electron–adsorbate coupling, but also enters together with the time-dependent adsorbate temperature in the prefactor of the rate $R(t)$. Thus, the dynamics of $R(t)$ is very different for either a low-temperature friction or a DIMET-type excitation. A dependence of η_e on electron temperature leads in any case to faster dynamics, as has been discussed for the desorption of NO from Pd(111) [32].

We have performed model calculations within the empirical and the generalized friction model in order to reproduce simultaneously the observed fluence dependence as well as the two-pulse correlation data. For the two-temperature model we have used material parameters for Pt reported in [62] ($g = 6.76 \times 10^{17}$ W K^{-1} m^{-3}, $\gamma = 748$ J K^{-2} m^{-3}, $\kappa_0(77\text{ K}) =$

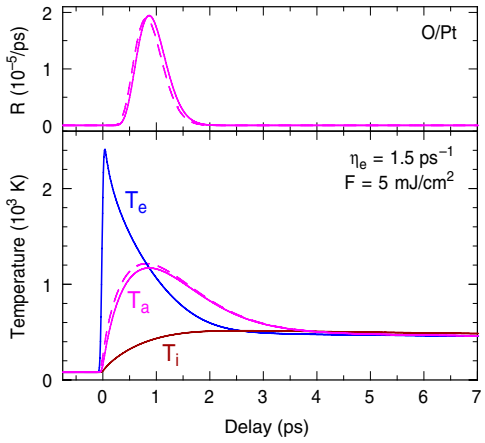

Figure 4. Time-dependence of electron temperature T_e, ion temperature T_i, adsorbate temperature T_a, and diffusion rate R as derived from the two-temperature and the empirical as well as the generalized electronic friction model for a constant electron friction $\eta_e = 1.5$ ps^{-1}, a laser pulse length of 50 fs, an absorbed laser fluence of 5 mJ cm^{-2}, and a diffusion barrier of $E_{dif} = 1.4$ eV. T_e and T_i are identical for both models. The solid magenta line show the results for T_a and R derived from the generalized friction model, while the dashed magenta line shows the results calculated within the empirical friction model.

71.6 W K^{-1} m^{-1}, Debye temperature $T_D = 240$ K). In this work the calculated electron temperature has been verified by comparing it with the dynamics of the transient electron distribution which has been observed by time-resolved photoelectron spectroscopy using a 1.5 eV pump pulse and a 42 eV probe pulse. These observations showed that the electron distribution is completely thermalized within 250 fs after the pump pulse. Thermal activated hopping has been observed at 275 K with a rate of 5×10^{-4} s^{-1}, which increases to 5×10^{-3} s^{-1} at 305 K [67]. From these experiments we estimate the diffusion barrier from step to terrace sites as $E_{dif} \approx 0.8$ eV, which is ≈0.3 eV larger than the barrier for hopping between terrace sites [68, 69]. The frustrated translation mode of O on Pt(111) has been observed by IR spectroscopy at a frequency of 1.2×10^{13} s^{-1} [70]. X-ray absorption spectroscopy of O/Pt(111) by Puglia *et al* [71] revealed a broad unoccupied resonance very close to the Fermi level, which has been assigned to an antibonding state due to hybridization of the O $2p_z$ level and the Pt 5d band. A second weaker and broader resonance centred at 8 eV above the latter has been assigned to the hybridization of the Pt 6sp and the O $2p_{xy}$ states. Thus, energy transfer to the oxygen atoms, which weakens the O–Pt bond, can be expected even at low electron temperatures and without a strong temperature dependence. This has been confirmed by recent *ab initio* calculations of the friction coefficient for atomic oxygen in the fcc hollow site on a flat Pt(111) surface [72]. The lateral friction for a fixed distance of the oxygen atom at low temperatures has been calculated to be $f = 2.5$ meV ps Å^{-2} ($\eta_e = 1.5$ ps^{-1}), which changes by less than 10% for temperatures of up to 3000 K.

Figure 4 shows the results of the model calculations for an excitation with a single 50 fs laser pulse. For an absorbed laser fluence of 5 mJ cm^{-2} the electron temperature rises up to 2200 K while the ion temperature remains below 500 K. The adsorbate temperature T_a and the diffusion rate R have been calculated for the empirical as well as for the generalized friction model using a constant electronic friction of $\eta_e = 1.5$ ps^{-1}. This results in dynamics of the adsorbate temperature, which is in between the dynamics of electron and ion temperature. The maximum adsorbate temperature of 1200 K is reached at about 800 fs after the pump pulse.

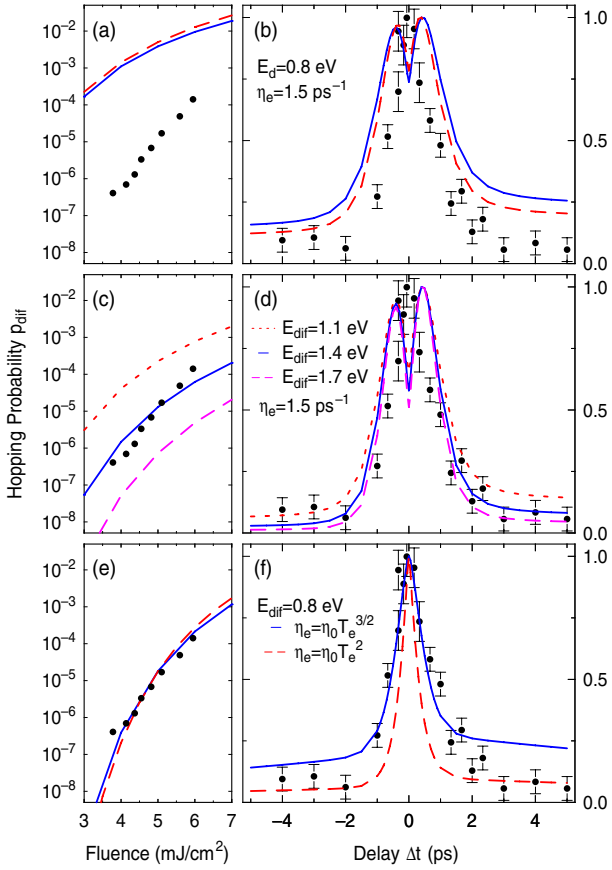

Figure 5. Calculated hopping probability p_{dif} (left) as a function of absorbed fluence and (right) as a function of time delay between two pump pulses. Experimental data are indicated by symbols. The two-pulse correlation traces are normalized to unity. (a) and (b) show the results of the empirical (dashed lines) and the generalized (solid line) friction model for $E_{\mathrm{dif}} = 0.8$ eV and $\eta_{\mathrm{e}} = 1.5$ ps^{-1}. (c) and (d) illustrate the influence of the diffusion barrier height on the results of the generalized friction model using a constant friction of $\eta_{\mathrm{e}} = 1.5$ ps^{-1}. The solid and dashed lines in (e) and (f) are the results for two different dependences of the friction coefficient on electron temperature.

The empirical and the generalized friction model show nearly identical results not only for T_{a}, but also for R. At first glance, the agreement for the latter is surprising, since the prefactor of the reaction rate is defined differently in both cases (equations (5) and (7)). However, the Boltzmann factor contributes mainly for temperatures for which E_{a}/kT is of the order of 10. For these temperatures the prefactor is comparable in both cases. The only qualitative difference appears in the two-pulse correlation shown in figure 5(b). The contrast between p_{dif} at zero and large delays is slightly smaller for the generalized friction model. This is mainly caused by the fact that the adsorbate temperature enters in the denominator of equation (7), which leads to a reduced rise of p_{dif} at small delays where the adsorbate temperature is large. Compared to the experimental data, however, the calculated hopping probabilities are too large by two to three orders of magnitude, and the strong nonlinearity of the fluence dependence cannot be reproduced for a diffusion barrier of $E_{\mathrm{dif}} = 0.8$ eV (figure 5(a)). On the other hand, the normalized two-pulse correlations are only slightly broader than observed in the experiment. This shows that the energy transfer time, which is associated with the friction

coefficient, is in the correct range. However, the huge discrepancy between the absolute values cannot be reduced by variation of the friction coefficient. A larger friction narrows the two-pulse correlation, but even further increases p_{dif}, while a smaller friction results in an even broader two-pulse correlation.

A rather good description of the observed fluence dependence and two-pulse correlation can be achieved if the diffusion barrier is arbitrarily increased. This is shown in figures 5(c) and (d), which display the results of the generalized friction model with fixed friction and varying diffusion barrier E_{dif}. With increasing E_{dif} the width of the two-pulse correlation narrows, and the fluence dependence becomes steeper since the variation of the Boltzmann factor in equation (7) becomes stronger the larger E_{dif} is compared to kT_{a}. The best agreement is achieved for $E_{\mathrm{dif}} = 1.4$ eV, which is, however, much larger than the barrier observed for thermally activated diffusion. It has been argued that the activation energy of the generalized friction model in equation (7) has to be regarded as *modified* activation energy, which exceeds the depth of the well, indicating the population of excited states [73]. However, this argument is not consistent with the assumption of the generalized friction model. In both the empirical as well as the generalized friction model, the binding of the adsorbate to the surface is approximated by a truncated oscillator potential of depth E_{a}, and the electronic excitation is represented by the friction coefficient. The main difference between both models is the handling of high-lying electronic states. While these are not covered by the empirical friction model, an electron-temperature-dependent friction is used in the generalized friction model in order to describe an (activated) population of an electronic state which cannot significantly be occupied at low temperatures. Thus, we have introduced an empirical dependence of the electronic friction on electron temperature in order to reproduce our data with a reasonable value for the diffusion barrier.

Figures 5(e) and (f) show the results of the generalized friction model using a diffusion barrier of $E_{\mathrm{dif}} = 0.8$ eV and a temperature dependence of the friction of the form $\eta_{\mathrm{e}} = \eta_0 T^x$ with $x = 3/2$ and 2. Indeed, this parametrization reproduces particularly well the high nonlinearity of the fluence dependence and results in a narrow two-pulse correlation even for a low barrier. The exact shape of the two-pulse correlation apparently depends on the analytic form of the assumed temperature dependence. For the chosen cases the two-pulse correlation is either somewhat smaller than the experimental one ($x = 2$) or does not reach the experimentally observed contrast ratio of p_{dif} between zero and large delays ($x = 3/2$). Nevertheless, these calculations demonstrate that a temperature-dependent friction can reproduce the main features of the experimental observations without choosing an unphysical barrier height. As discussed in [39], the temperature-dependent friction results in a different dynamics of the adsorbate temperature. It shows only a fast rise-time and cools down slowly since the coupling strength rapidly decreases with electron temperature. Nevertheless, the hopping rate R has dynamics on the timescale of one picosecond since $\eta_{\mathrm{e}}(T_{\mathrm{e}}(t))$ enters into its prefactor (equation (7)). The dependence of R on electron temperature via η_{e} is responsible for the narrow two-pulse correlation shown in figure 5(f), which has its maximum at zero delay.

The dip of the calculated hopping probability around zero delay in figure 5(b) and (d) results from the competition between electron–phonon coupling and diffusive hot-electron transport [74]. The first tends to localize the heat at the surface while the latter is responsible for the distribution of the heat into the bulk. For delays which are small compared to the electron–phonon coupling time, the enhanced electron temperature leads to a stronger temperature gradient between surface and bulk. This results in a faster diffusion of the hot electrons into the bulk. Thus, the maximum ion temperature at the surface is reduced for small delays between the pump pulses. The more the dynamics of adsorbate and ion temperature become similar, i.e. for small friction, the more this reduction affects the

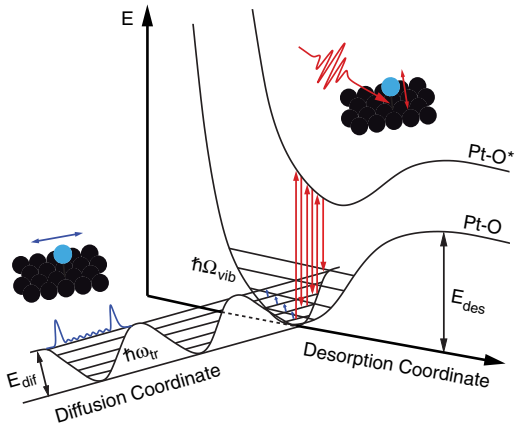

Figure 6. Schematic potential energy scheme for an indirect excitation of diffusion by anharmonic coupling with the Pt–O vibration.

adsorbate temperature. The hopping probability should be even more sensitive to this effect since it depends exponentially on the adsorbate temperature. This consequence of the two-temperature model has been experimentally verified for the surface temperature of the substrate in time-resolved reflectivity measurements on various metal surfaces [74], but has not yet been observed in femtosecond surface photochemistry experiments. Even the laser-induced desorption of CO from Ru(0001) [18], which is believed to be mediated almost solely by substrate phonons, does not show this proposed reduction. This indicates that the full reaction dynamics are in fact more complicated than can be described by a time-dependent adsorbate temperature coupled by a single friction coefficient.

4. Discussion

The model calculations show that the experimental data can only be reproduced with a reasonable value for the diffusion barrier if we assume a dependence of the friction on electron temperature. However, the electronic structure of O on Pt(111) and the *ab initio* calculations do not support a temperature dependence of the electronic excitation of low-energy vibrational modes. Thus, the question arises of whether the pathway of the energy transfer to the diffusive motion is in fact more complicated than a direct coupling of the electronic excitation to the frustrated translation mode. For this reason we suggest an indirect excitation mechanism which requires an effective dependence of η_e on electron temperature within in the description of the friction model. This mechanism is sketched in figure 6. It assumes a primary electronic excitation of the O–Pt stretch vibration, which indirectly excites the frustrated translation via anharmonic coupling. Since the anharmonicity of vibrations generally increases with amplitude, the corresponding coupling strength increases with the vibrational temperature of the O–Pt stretch. Its energy (60 meV) is only slightly higher than the energy of frustrated O–Pt translations (50 meV) [70]. Therefore, many quanta of the stretch vibration mode need to be excited by repetitive electronic excitation cycles before the vibrational motion can couple efficiently to the lateral mode and before the diffusion barrier of ∼0.8 eV can be overcome. If such a scenario is described by a single coupling strength, it will depend effectively on electron temperature, while the primary electronic excitation of the O–Pt stretch vibrations could still be mediated by a constant electronic friction η_e, as illustrated in figure 7.

This model of an indirect excitation mechanism of lateral motion is motivated by recent STM experiments of Komeda *et al* [75] and Pascual *et al* [76], who found a threshold energy

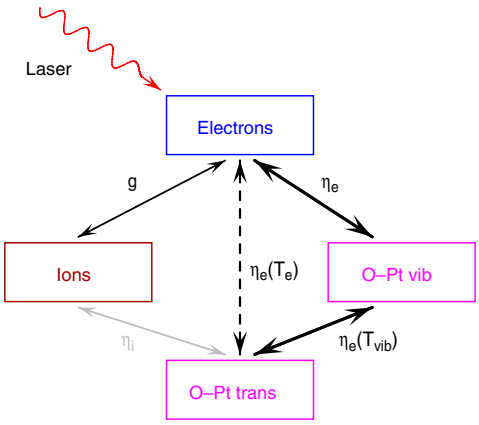

Figure 7. Scheme of the energy transfer from the optical excitation of the electrons to the frustrated translation mode which initiates the diffusive motion of the oxygen atoms. An effective dependence of the electronic friction η_e on electron temperature T_e can result from an indirect excitation by anharmonic coupling between the O–Pt stretch and the O–Pt translation mode.

for inducing diffusion of CO/Pd(110) and NH_3/Cu(100) by inelastic electron tunnelling, which coincides with the internal CO and NH stretch vibration respectively. The lateral motion is shown to be initiated by anharmonic coupling between the high-frequency internal and the low-frequency frustrated translation mode. For these systems even one quantum of internal vibrational energy exceeds the diffusion barrier. Thus, an indirect excitation of lateral motion is possible, even if the low current in the STM experiments of <0.05 e^- ps^{-1} inhibits ladder climbing due to the short lifetimes of the vibrational modes on metal surfaces. The importance of the anharmonic coupling has been demonstrated in the experiments of Komeda *et al* by comparing CO/Pd(110) and CO/Cu(110). Even if the diffusion barrier of the latter is smaller by a factor of two, no lateral hopping by excitation of the internal stretch can be observed. This has been explained by the different strength of the anharmonic coupling [77, 78], which is larger by a factor of more than 20 for CO/Pd(110). The anharmonic coupling $\hbar\delta\omega$ of vibrational modes can be estimated from the temperature dependence of their frequency and linewidth [65]. If applied to the temperature dependent IR data of Engström *et al* [70], it results in $\hbar\delta\omega \approx 2$ meV for the O–Pt stretch vibration. This is comparable to CO/Pd(110), and Engström *et al* mentioned in [79] that a relevant decay mechanism for the O–Pt stretch vibration is the excitation of a parallel adsorbate mode by anharmonic coupling, which increases with temperature, as has been shown in a theoretical work for O on Ni(111) [80].

The proposed mechanism suggests a stronger electronic coupling to the O–Pt stretch vibration than to the frustrated translation. Anisotropic electronic friction has been found, for example, for H_2 on Cu(111) and N_2 on Ru(0001) [34], which implies an initially strong adsorbate–substrate vibration perpendicular to the surface. For oxygen on a flat Pt(111) surface, however, the electronic friction calculated for the direction perpendicular to the surface is only 20% larger than for the lateral direction [72]. On the other hand, this difference does not need to be very large in order to result in a temperature-dependent coupling strength. In any case, the anharmonic coupling of the stretch vibration provides an additional pathway for the energy transfer, which becomes more efficient with increasing excitation density. Thus, this mechanism should be included in an accurate description of the energy transfer dynamics. The anisotropy of the friction may also be different for oxygen atoms at step sites due to their different coordinations, which could enhance the importance of the anharmonic coupling in our case.

5. Conclusion

Femtosecond-laser-induced diffusion of atomic oxygen on a vicinal Pt(111) surface has been used to study the energy transfer dynamics from the optical excitation to the frustrated translation for a strongly chemisorbed atomic adsorbate. The experimental results have shown that the diffusive motion is driven by the laser-excited electrons of the metallic substrate. The extreme nonlinear dependence of the hopping rate on laser fluence, however, indicates that the energy transfer mechanism is more complicated than for the case of desorption. This is reflected by the fact that a consistent description of the experimental data within the generalized electronic friction model cannot be achieved with a constant electronic friction and a reasonable value for the diffusion barrier, but requires the introduction of a temperature-dependent electronic friction coefficient. We suggest that this temperature dependence appears due to the neglect of the coupling between different vibrational modes. The proposed mechanism of an indirect excitation by anharmonic coupling to the O–Pt stretch introduces a coupling which depends on excitation density and would therefore explain the observed effective dependence of the electronic friction on electron temperature.

Acknowledgments

K Stépán is credited for her excellent experimental contribution to the work presented here. We thank A C Luntz and M Persson for valuable discussions. This work was supported by the Deutsche Forschungsgemeinschaft through SPP 1093, and GK 790, the German–Israel Science Foundation and the Marburg Centre for Optodynamics.

References

[1] Menzel D and Gomer R 1964 *J. Chem. Phys.* **41** 3311
[2] Redhead P A 1964 *Can. J. Phys.* **42** 886
[3] Zhou X L, Zhu X Y and White J M 1991 *Surf. Sci. Rep.* **13** 73
[4] Weik F, de Meijere A and Hasselbrink E 1993 *J. Chem. Phys.* **99** 682
[5] Gadzuk J W 1996 *Laser Spectroscopy and Photo-Chemistry on Metal Surfaces Part II* ed H L Dai and W Ho (Singapore: World Scientific) pp 897–942
[6] Prybyla J A, Heinz T F, Misewich J A, Loy M M T and Glownia J H 1990 *Phys. Rev. Lett.* **64** 1537
[7] Budde F, Heinz T F, Loy M M T, Misewich J A, Derougemont F and Zacharias H 1991 *Phys. Rev. Lett.* **66** 3024
[8] Prybyla J A, Tom H W K and Aumiller G D 1992 *Phys. Rev. Lett.* **68** 503
[9] Kao F J, Busch D G, Dacosta D G and Ho W 1993 *Phys. Rev. Lett.* **70** 4098
[10] Kao F J, Busch D G, Cohen D, Dacosta D G and Ho W 1993 *Phys. Rev. Lett.* **71** 2094
[11] Misewich J A, Heinz T F, Kalamarides A, Höfer U and Loy M M T 1994 *J. Chem. Phys.* **100** 736
[12] Deliwala S, Finlay R J, Goldman J R, Her T H, Mieher W D and Mazur E 1995 *Chem. Phys. Lett.* **242** 617
[13] Busch D G, Gao S W, Pelak R A, Booth M F and Ho W 1995 *Phys. Rev. Lett.* **75** 673
[14] Busch D G and Ho W 1996 *Phys. Rev. Lett.* **77** 1338
[15] Struck L M, Richter L J, Buntin S A, Cavanagh R R and Stephenson J C 1996 *Phys. Rev. Lett.* **77** 4576
[16] Finlay R J, Her T H, Wu C and Mazur E 1997 *Chem. Phys. Lett.* **274** 499
[17] Her T H, Finlay R J, Wu C and Mazur E 1998 *J. Chem. Phys.* **108** 8595
[18] Bonn M, Funk S, Hess C, Denzler D N, Stampfl C, Scheffler M, Wolf M and Ertl G 1999 *Science* **285** 1042
[19] Eichhorn G, Richter M, Al-Shamery K and Zacharias H 1999 *J. Chem. Phys.* **111** 386
[20] Cai L, Xiao X D and Loy M M T 2000 *Surf. Sci.* **464** L727
[21] Cai L, Xiao X D and Loy M M T 2001 *J. Chem. Phys.* **115** 9490
[22] Quinn D P and Heinz T F 2003 *J. Vac. Sci. Technol.* A **21** 1312
[23] Denzler D N, Frischkorn C, Hess C, Wolf M and Ertl G 2003 *Phys. Rev. Lett.* **91** 226102
[24] Wagner S, Frischkorn C, Wolf M, Rutkowski M, Zacharias H and Luntz A C 2005 *Phys. Rev.* B **72** 205404
[25] Feulner P and Menzel D 1995 *Laser Spectroscopy and Photo-Chemistry on Metal Surfaces Part II* ed H L Dai and W Ho (Singapore: World Scientific) pp 627–84
[26] Hasselbrink E 1990 *Chem. Phys. Lett.* **170** 329
[27] Misewich J A, Heinz T F and Newns D M 1992 *Phys. Rev. Lett.* **68** 3737

[28] Newns D M, Heinz T F and Misewich J A 1991 *Prog. Theor. Phys. Suppl.* **106** 411
[29] Budde F, Heinz T F, Kalamarides A, Loy M M T and Misewich J A 1993 *Surf. Sci.* **283** 143
[30] Misewich J A, Heinz T F, Weigand P and Kalamarides A 1996 *Laser Spectroscopy and Photo-Chemistry on Metal Surfaces Part II* ed H L Dai and W Ho (Singapore: World Scientific) pp 764–826
[31] Head-Gordon M and Tully J C 1995 *J. Chem. Phys.* **103** 10137
[32] Brandbyge M, Hedegard P, Heinz T F, Misewich J A and Newns D M 1995 *Phys. Rev.* B **52** 6042
[33] Springer C and Head-Gordon M 1996 *Chem. Phys.* **205** 73
[34] Luntz A C and Persson M 2005 *J. Chem. Phys.* **123** 074704
[35] Bohnen K P, Kiwi M and Suhl H 1975 *Phys. Rev. Lett.* **34** 1512
[36] Nourtier A 1977 *J. Physique* **38** 479
[37] Bartels L, Wang F, Moller D, Knoesel E and Heinz T F 2004 *Science* **305** 648
[38] Stépán K, Güdde J and Höfer U 2005 *Phys. Rev. Lett.* **94** 236103
[39] Stépán K, Dürr M, Güdde J and Höfer U 2005 *Surf. Sci.* **593** 54
[40] Backus E H G, Eichler A, Kleyn A W and Bonn M 2005 *Science* **310** 1790
[41] Wang H, Tobin R G, Lambert D K, DiMaggio C L and Fisher G B 1997 *Surf. Sci.* **372** 267
[42] Gee A T and Hayden B E 2000 *J. Chem. Phys.* **113** 10333
[43] Gland J L, Sexton B A and Fisher G B 1980 *Surf. Sci.* **95** 587
[44] Winkler A, Guo X, Siddiqui H R, Hagans P L and Yates J T 1988 *Surf. Sci.* **201** 419
[45] Gambardella P, Šljivančanin Ž, Hammer B, Blanc M, Kuhnke K and Kern K 2001 *Phys. Rev. Lett.* **87** 056103
[46] Shen Y R 1989 *Annu. Rev. Phys. Chem.* **40** 327
[47] Reider G A and Heinz T F 1995 *Photonic Probes of Surfaces* ed P Halevi (Amsterdam: North-Holland) pp 3–66
[48] Lüpke G, Bottomley D J and Vandriel H M 1994 *J. Opt. Soc. Am.* B **11** 33
[49] Kratzer P, Pehlke E, Scheffler M, Raschke M B and Höfer U 1998 *Phys. Rev. Lett.* **81** 5596
[50] Raschke M B and Höfer U 1999 *Phys. Rev.* B **59** 2783
[51] Reutt-Robey J E, Doren D J, Chabal Y J and Christman S B 1990 *J. Chem. Phys.* **93** 9113
[52] Feibelman P J, Esch S and Michely T 1996 *Phys. Rev. Lett.* **77** 2257
[53] Campbell C T, Ertl G, Kuipers H and Segner J 1981 *Surf. Sci.* **107** 220
[54] Zhu X Y, Hatch S R, Campion A and White J M 1989 *J. Chem. Phys.* **91** 5011
[55] Watanabe K, Sawabe K and Matsumoto Y 1996 *Phys. Rev. Lett.* **76** 1751
[56] Bauer M, Pawlik S, Burgermeister R and Aeschlimann M 1998 *Surf. Sci.* **404** 62
[57] Ogawa S, Nagano H and Petek H 1999 *Phys. Rev. Lett.* **82** 1931
[58] Wolf M, Hotzel A, Knoesel E and Velic D 1999 *Phys. Rev.* B **59** 5926
[59] Anisimov S I, Kapeliovich B L and Perelman T L 1974 *Sov. Phys.—JETP* **39** 375
[60] Fann W S, Storz R, Tom H W K and Bokor J 1992 *Phys. Rev. Lett.* **68** 2834
[61] Fann W S, Storz R, Tom H W K and Bokor J 1992 *Phys. Rev.* B **46** 13592
[62] Lei C, Bauer M, Read K, Tobey R, Liu Y, Popmintchev T, Murnane M M and Kapteyn H C 2002 *Phys. Rev.* B **66** 245420
[63] Guo H, Saalfrank P and Seideman T 1999 *Prog. Surf. Sci.* **62** 239
[64] Persson B N J and Persson M 1980 *Solid State Commun.* **36** 175
[65] Persson B N J and Ryberg R 1985 *Phys. Rev. Lett.* **54** 2119
[66] Tully J C, Gomez M and Head-Gordon M 1993 *J. Vac. Sci. Technol.* A **11** 1914
[67] Stépán K 2006 *Dissertation* Philipps-Universität Marburg
[68] Wintterlin J, Schuster R and Ertl G 1996 *Phys. Rev. Lett.* **77** 123
[69] Bogicevic A, Strömquist J and Lundqvist B I 1998 *Phys. Rev.* B **57** R4289
[70] Engström U and Ryberg R 1999 *Phys. Rev. Lett.* **82** 2741
[71] Puglia C, Nilsson A, Hernnas B, Karis O, Bennich P and Mårtensson N 1995 *Surf. Sci.* **342** 119
[72] Luntz A C 2005 private communications
[73] Denzler D N, Frischkorn C, Wolf M and Ertl G 2004 *J. Phys. Chem.* B **108** 14503
[74] Bonn M, Denzler D N, Funk S, Wolf M, Wellershoff S S and Hohlfeld J 2000 *Phys. Rev.* B **61** 1101
[75] Komeda T, Kim Y, Kawai M, Persson B N J and Ueba H 2002 *Science* **295** 2055
[76] Pascual J I, Lorente N, Song Z, Conrad H and Rust H P 2003 *Nature* **423** 525
[77] Persson B N J and Ueba H 2002 *Surf. Sci.* **502** 18
[78] Ueba H, Mii T, Lorente N and Persson B N J 2005 *J. Chem. Phys.* **123** 084707
[79] Engström U and Ryberg R 2000 *J. Chem. Phys.* **112** 1959
[80] Ariyasu J C and Mills D L 1984 *Phys. Rev.* B **30** 507